CONFIGURATION AND TRAJECTORY OF HYPERSONIC TRANSPORT WITH AEROTHERMODYNAMIC CONTROL

ICAS-86-2.10.3

Y. Aihara, Department of Aeronautics,
Faculty of Engineering, University of Tokyo,
S. Nomura, First Aerodynamics Division,
National Aerospace Laboratory,
H. Minakuchi, A. Murakami and N. Sudani,
Department of Aeronautics, Faculty of Engineering,
University of Tokyo.

Abstract

Aerodynamics of an HST with a range of 16,000km has been studied on the assumption that the Mach number at the beginning of horizontal cruising is 7. Orbit analysis has been made through modeling of the relations of air density and sound velocity vs. altitude and of lift-to-drag ratio and specific impulse vs. Mach number, revealing that the aerodynamic characteristic effective to increase the payload and shorten the flight time is the lift-to-drag ratio under hypersonic flight. The results of a wind tunnel test of the HST model at Mach number 7 have shown that the geometry of the model almost satisfies the aerodynamic performance assumed in said orbit analysis. An experiment for heating of the air stream beneath the afterbody suggests the possibility of improving the lift-to-drag ratio. Applicability of the heat addition to a real HST remains a problem to be thrashed out.

I. Introduction

Hypersonic Transport, which will be able to fly halfway around the Earth in about 2 or 3 hours, is expected to promote new developments in aircraft transport and at the same time to be applicable as a means of space travel. Feasibility of HST has been shown even in the studies reported up to the early 1970s[1]~[8].

It would be significant to examine an HST plan based on more advanced aircraft technology of today.

This paper discusses an economical cruising type HST from an aerodynamic point of view as follows :

(1) Supposing that the HST flies halfway around the Earth in a quasi-stationary equilibrium flight, the relations between variations in the velocity, Mach number, weight etc. along the anticipated flight path and the aerodynamic characteristics of the HST are investigated.

(2) The basic geometry of the HST with desirable aerodynamic characteristics is experimentally and numerically investigated.

(3) The effect of heating the air stream beneath the afterbody as a means to improve and control the aerodynamic characteristics under hypersonic cruising is examined.

II. Flight Path and Aerodynamic Characteristics

The equilibrium flight is expressed by the following equations.

$$T = D + mg\sin\theta \tag{1}$$

$$mg\cos\theta = L \tag{2}$$

where T : thrust; D : drag; L : lift; m : HST mass; g : gravitational acceleration; and θ : path angle.
Writing

$$T = -VgI_{sp}\frac{dm}{ds} \tag{3}$$

(1) and (2) can be combined into

$$-\frac{dm}{m} = \frac{1}{I_{sp}}\left(\frac{\cos\theta}{\left(\frac{L}{D}\right)} + \sin\theta\right)\frac{ds}{V} \tag{4}$$

where V is the velocity along the path s, and I_{sp} is specific impulse. Integrating (4) with respect to the nondimensional distance ξ along the Earth surface ($ds\cos\theta = Rd\xi$, R : range) instead of using s, yields the mass change from the time of take-off (index 0) as follows :

$$\frac{m}{m_0} = \left\{1 - \frac{R}{2^{\frac{3}{2}}}\left(\frac{\rho_0}{w_0}\right)^{\frac{1}{2}}\left(\frac{1}{I_{sp}}\right)_0\int_0^{\xi}\frac{1}{\left(\frac{I_{sp}}{I_{sp_0}}\right)}\cdot\left(\frac{1}{\left(\frac{L}{D}\right)} + \tan\theta\right)\cdot\left(\frac{\frac{\rho}{\rho_0}C_L}{\cos\theta}\right)^{\frac{1}{2}}d\xi\right\}^2 \tag{5}$$

where Wo : the wingloading at take-off; ρ : air density; and C_L : lift coefficient.

From (2) it follows that

$$V = \sqrt{2\frac{W_0}{\rho_0}\frac{m}{m_0}\frac{\cos\theta}{\left(\frac{\rho}{\rho_0}\right)C_L}} \tag{6}$$

and the Mach number M can be expressed by

$$M = \frac{V}{a} \tag{7}$$

where a is sound velocity.

Flight time t can be determined from

$$t = \int_0^1 \frac{Rd\xi}{V\cos\theta} \qquad (8)$$

Altitude h can be determined from

$$h = \int_0^{\xi} R\tan\theta d\xi \qquad (9)$$

Thus when the variations of ρ and a with h and of L/D and I_{sp} with M are known and θ is controlled, the relationship between flight path and aerodynamic characteristics can be investigated using the system of (5)~(9). As for the values of ρ and a, the Standard Atmospheric Table is referred to. As for the I_{sp}-M relation, available data will be employed[5]. In view of its aerodynamic importance, the link between the L/D-M relation and the results of the study are analyzed on several cases indicated in Figure 1. Case 1, which deals with the cruising performance of the conventional aircrafts, might be called an ideal state[9]. Case 2 shows an anticipated HST performance and Case 3 does a slightly inferior performance.

Meanwhile θ is assumed as follows : after take-off the HST climbs up at θ_a = 30°; at the Mach number initially set, i.e., Mc, it goes into horizontal flight (θ = 0°) and, reaching a point above the destination, it descends at $\tan\theta_d = -0.1$ ($\theta_d = -5°40'$).

Except in time of descent, a powered flight is considered. C_L is set at 0.15 (see Figure 10). The other necessary data are given in Table 1.

Figures 2~5 respectively indicate the variations of altitude, velocity, Mach number and mass with ξ, which have been obtained for M_c = 7 in cases 1 ~ 3 (①~③) and for M_c = 6 in case 3 (③'), of Figure 1. Figure 6 magnifies the state of ascent and descent of the HST for M_c = 7 in case 2.

From the results obtained under the above assumptions, it can be seen that the cruising altitude is about 30km and is a little higher for M_c = 7 than for M_c = 6. Mc is attained when the cruising altitude is reached; the velocity amounts to 2.20 km/s at M_c = 7 and to 1.93km/s at M_c = 6. Thereafter the flight continues up to a point above the destination with slight deceleration.

The effects of L/D and M_c emerge most prominently with respect to mass change and flight time. Mass ratios m_1/m_0 at landing are respectively 0.635, 0.530, 0.438 and 0.418 for ①~③'. Therefrom it follows that an increased L/D under hypersonic flight will be important for the purpose of increasing the HST payload. The flight times will be respectively 141.3, 147.9, 155.4 and 175.9 minutes for ①~③'. Therefrom it is known how important for the purpose of reducing the flight time of the HST are an increased L/D under hypersonic flight and a higher Mach number to be initially set.

Figure 7 is a sensitivity analysis about the data on ②. From Figure 7(a) it is seen that an increase in I_{sp} and L/D will be the most effective to increase the payload, followed by an increase in M_c. It is less sensitive to C_L, W_o or θ_a. The payload decrease is sensitive to an increase in R. Figure 7(b) shows that an increase in M_c is the most effective to reduce the required flight time followed by those in θ_a, I_{sp} and L/D. It is less sensitive to C_L and W_o. C_L is important for setting the flight height.

III. Aerodynamic Characteristics of HST

One of the important things in designing the cruising type HST is the setting of the Mach number for horizontal flight. In this study M_c = 7 is set as a reasonable target value, considering the scope of available data on the prospective ramjet and the thermal reaction of the atmospheric molecules in hypersonic flight. As a result of preliminary investigations about the basic form of a spiked delta wing, an initial configuration as illustrated in Figures 8 and 9 has been proposed as a subject to be studied. The body is sharply pointed, slender in section with round top and flat bottom. The wing is a delta wing swept-back to 65° with a strake wing swept-back to 83°, the angle of attaching to the plane axis being 10°. The upper line of the body is defined as the plane axis. The angle of attack, α, is measured from the axis. Behind the wing comes a plate afterbody fitted at -5° to the plane axis. Two fences are fitted parallel to the plane axis beneath the wing to hold a pressurized gas in between them. As suggested by the analysis in II, the aerodynamic characteristics under hypersonic flight is essential to the HST performance. Therefore an experiment on said configuration has been done in the hypersonic wind tunnel (M = 7 Reynolds number based on the model length, Re, = $0.8\sim3.2\times10^6$) of 50cm in the diameter of the measuring section at National Aerospace Laboratory; for details of the wind tunnel, see reference 11. Figure 10 summarizes the results of the wind tunnel test at Re = 3.2×10^6 together with the results of Newtonian flow simulation analysis based on panel division and its boundary layer correction analysis.

C_L increases with the angle of attack α from -10° to 10°. C_D has the minimum value near α = -7° and tends to increase in the positive range of α. C_m is the pitching moment coefficient around the tip. $(L/D)_{max}$ is 2.8 when $R_e = 0.8\times10^6$ and increases with Re. In Figure10(b), $(L/D)_{max}$ = 3.6 and C_L = 0.15 are obtained at α = 2°. The aerodynamic center is estimated to be located at 60.4% of the body length from the tip in this state. These data approximately correspond to those used in the analysis in case ② mentioned in II. Though the effect of the fences is not apparent in Figure 10, it will be discussed later

in relation to the surface flow patterns. From the Schlieren photograph (Figure 11), it can be seen that the shock wave is not so strong and the flow attaches to the surface. Oil flow patterns reveal that the parallel flow is established along the lower surface as a whole at $\alpha = 2°$ without fences, and the inflow downstream of the junction of the strake and the main wing and the outflow near the wingtip are noticed (Figure 12(a)). The fence generates new inflow near the leading edge but remarkable changes are not observed except that the outflow near the wingtip is improved (Figure 12(b)). The fences are expected to introduce high pressure air into propulsion system without disturbing the ambient flow field. The flow on the upper surface is observed to be considerably three-dimensional and the behaviour of viscous flow associated with the pressure distribution seems important for detailed discussions (Figures 12(c) and(d)). Though the primary estimate of the characteristics in Figure 10 can be done by Newtonian flow simulation analysis and the viscous correction, more elaborate method of analysis would be necessary for detailed design.

Similar tests are in progress for improving the performance by modifying the geometry.

IV. Control of Aerodynamic Characteristics by Heating of Stream Beneath Afterbody

An idea has been suggested of increasing the lift and decreasing the drag by elevating the static pressure of a supersonic stream flowing beneath the HST afterbody through heating[7],[12].

Putting the inclination angle of the model tip to the air stream and that of the afterbody to the air stream respectively as θ_1 and $-\theta$, the areas of the main wing and the afterbody respectively as A_1 and A, the static pressures acting on the main wing and on the afterbody respectively as P_1 and P_4, and the increment of P_4 due to heat addition as ΔP_4, the primary contribution of the heated stream to the lift-to-drag ratio will be expressed by

$$\frac{L}{D} = \left(\frac{L}{D}\right)_0 \left\{1 + \left(\frac{\cos\theta}{\cos\theta_1 + \left(\frac{P_4}{P_1}\right)_0 \frac{A}{A_1}\cos\theta} + \frac{\sin\theta}{\sin\theta_1 - \left(\frac{P_4}{P_1}\right)_0 \frac{A}{A_1}\sin\theta}\right) \cdot \frac{A}{A_1}\frac{\Delta P_4}{P_1}\right\} \quad (10)$$

where $(\quad)_0$ shows the value without heating.

To determine how effectively the idea can be realized is the problem to be solved hereafter. In this study an experiment has been undertaken of heating the air stream flowing along the surface of the plane body upstream of the afterbody, using a wind tunnel model (Figure 13) on a reduced scale with near-similarity to the model illustrated in Figure 8, installed in the hypersonic wind tunnel (M = 7) at Department of Aeronautics, Faculty of Engineering, of the University of Tokyo. An electric heater , set in the body is used to control the surface temperature T_W. As the electricity supply is switched on just before the model is put in the flow, the surface temperature increases locally (Figure 14). The temperature distribution is unchanged during the measurement. In the wind tunnel, T_W can be set at about 1.6 times T_O by holding the stagnation temperature T_O at low value. Figure 15 shows the ratio of the static pressure P_1 beneath the main wing and the static pressure P_4 beneath the afterbody as a function of T_W/T_O. It is seen how P_4/P_1 increases with an increase of T_W and then decreases, but the measured value is found considerably lower than the value estimated by Euler equation. If we substitute the result $(P_4/P_1)_0 = 0.42$ and $\Delta P_4/P_1 = 0.25$ into (10) and use the values $A/A_1 = 3/8$ and $\theta/\theta_1 = 1/2$ for the HST model discussed in III, $(L/D)_{max}$ is expected to increase from 3.6 to 4.1 by the aerothermodynamic control.

Practical application of the idea to the aerodynamic control of a real HST would have to be undertaken considering the process of heat addition and the scale effect.

The propulsion system is not involved in the present study and further study is needed for the integrated configuration. The shock-boundary layer interaction as one of the important problems associated with engine installation is investigated separately, and the importance of three-dimensional boundary layer separation and the generation of longitudinal vortices are revealed experimentally[13].

V. Conclusions

1. An analysis of equilibrium flight of HST with $M_C = 7$ reveals that an effective aerodynamic measure to raise the payload and reduce the flight time will be an increase in the lift-to-drag ratio in hypersonic flight.

2. A wind tunnel test of HST model at M = 7 has been done, yielding a lift-to-drag ratio of 3.6 and a lift coefficient of 0.15. A Newtonian flow simulation analysis has been found useful for primary estimation of the performance of HST model. With reference to the analysis 1 in the above, the HST model has been confirmed as a candidate of the basic configuration of the HST.

3. Possibility of improving the lift-to-drag ratio by heating the stream beneath the afterbody has been proved. A number of problems remain to be solved before application to the real HST, such as the boundary layer, and the scale effect.

4. Summing up the results in 1 and 2 above and assuming an HST of $M_C = 7$ and

length of fuselage equal to Boeing 747 (70m), realization of a transport which can fly halfway around the Earth in about 2½ hours carrying a payload of about 30 tons is found feasible, provided the dead-weight is estimated at 40% of the take-off weight.

Acknowledgements - The authors would like to express their thanks to Director Dr. I. Wada and Mr. K. Hozumi at First Aero-dynamics Division, NAL, for their helpful discussions and cooperation in wind tunnel testing. Their thanks are also due to Mr. H. Koyama and Mr. T. Okunuki at Dept. of Aeron., Univ. Tokyo, for their assistance and cooperation during the course of this study, and to Miss T. Munakata for typing the manuscript.

References

1. D.M. Ashford, Boost-Glide Vehicles for Long Range Transport. Jour. Roy. Aeron. Soc. 69, 448-458 (1965).

2. R.H. Petersen, T.J. Gregory and C.L. Smith, Some Comparisons of Turbo-ramjetpowered Hypersonic Aircraft for Cruise and Boost Missions. J. Air-craft 3, 308-405 (1966).

3. A.J. Eggers, Jr., R.H. Petersen and N.B. Cohen, Hypersonic Aircraft Tech-nology and Applications. Astron. and Aeron. June, 30-41 (1970).

4. T.J. Gregory, L.J. Williams and D.E. Wilcox, The Airbreathing Launch Vehicle for Earth Orbit Shuttle-Performance and Operation. AIAA Advanced Space Transportation Meeting Cocoa Beach, Florida, AIAA-70-270 (1970).

5. M.W. Hunter II and D.W. Fellenz, The Hypersonic Transport - The Technology and The Potential. AIAA 7th Annual Meeting and Technical Display, Houston, Texas, AIAA-70-1218 (1970).

6. R.H. Miller, Some Air Transportation Concepts for the Future, Fourteenth Lanchester Memorial Lecture. The Aeron. Jour. Roy. Aeron. Soc. 75, 431-456 (1971).

7. K. Enkenhus and J.F. Wendt (ed), Aerodynamic Problems of Hypersonic Vehicles. AGARD-LS-42, Vol. 1 (1972).

8. E.M. Repic, G.A. Olson and R.J. Milliken, A Methodology for Boost-Glide Transport Technology Planning. NASA CR-2346 (1974).

9. D. Küchemann, The Aerodynamic Design of Aircraft. Pergamon Press, Oxford (1978).

10. P.J. Conchie, A Horizontal Take-Off and Landing Satellite Launcher of Aerospace Plane (HOTOL).Jour. British Interplanetary Soc.38,387-390 (1985).

11. S. Nomura, N. Hashimoto, A. Yoshizawa and K. Hozumi, The Viscous Flow over Axisymmetric Body with and without Angle of Attack at M = 7. Proc. 10th Int. Symp. Space Tech. Sci., Tokyo, 443-447 (1973).

12. J. Zierep, Theory of Flows in Compressible Media with Heat Addition. AGARD-AG-191 (1974)

13. A. Murakami, Study on Three-Dimensional Shock-Boundary Layer Interaction. Master Thesis, Graduate School of Dept. Aeron., Univ. Tokyo (1986) (in Japanese).

R	range	16,000km
W_0	take-off wingloading	700kg/m^2
I_{spo}	take-off specific impulse	5000s
ρ_0	air density at sea level	1/8kgs^2/m^4

Table 1. Data of the analysis.

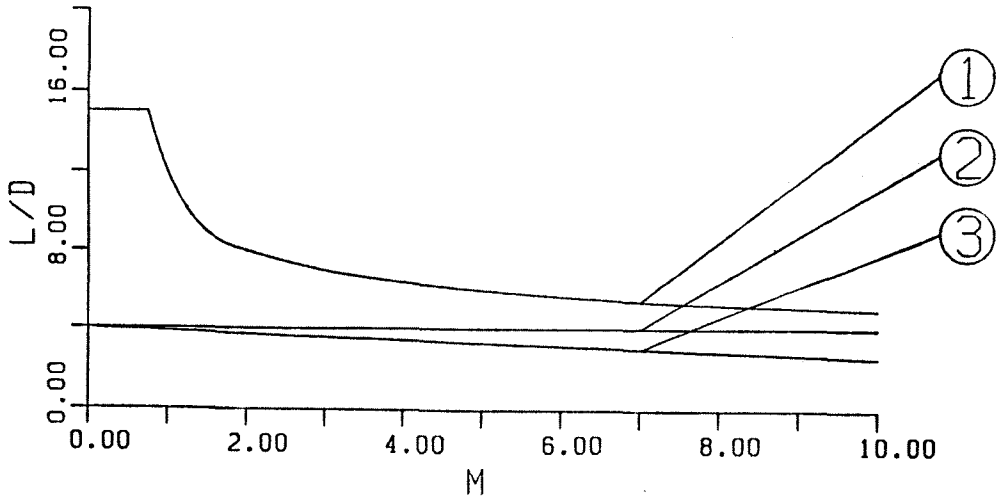

Fig. 1 Various models of lift-to-drag ratios vs. Mach number.

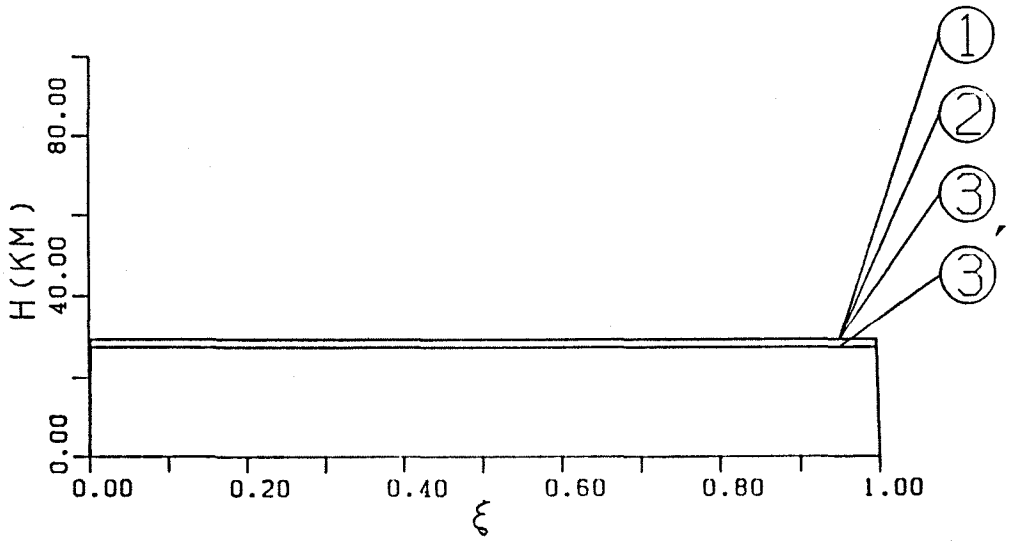

Fig. 2 Flight height.

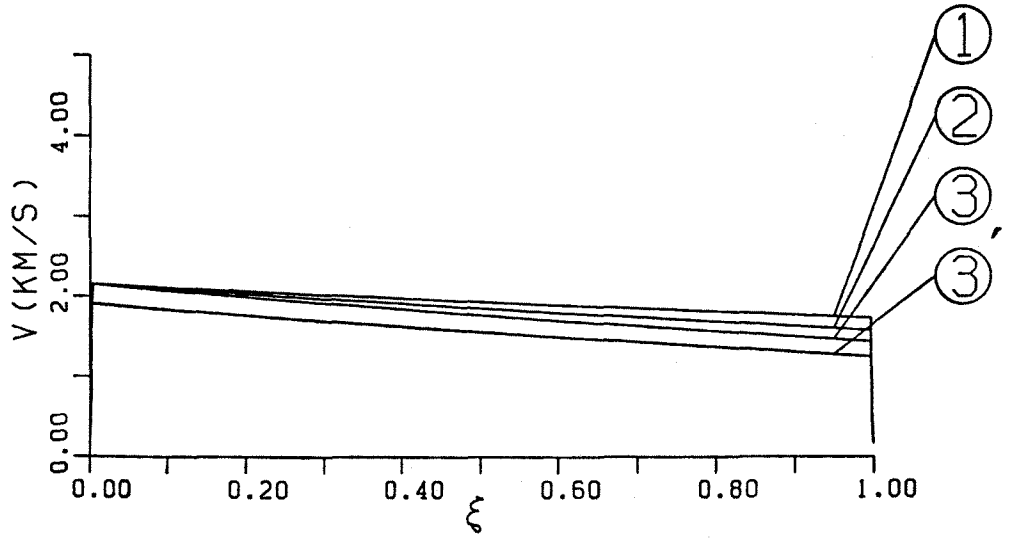

Fig. 3 Variations of flight speeds vs. nondimensional distance.

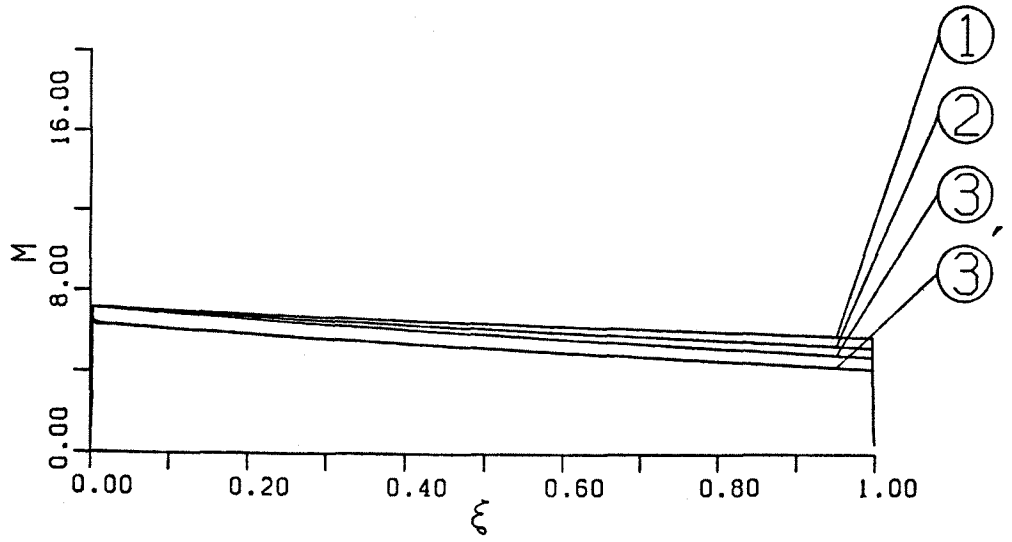

Fig. 4 Variations of Mach numbers vs. nondimensional distance.

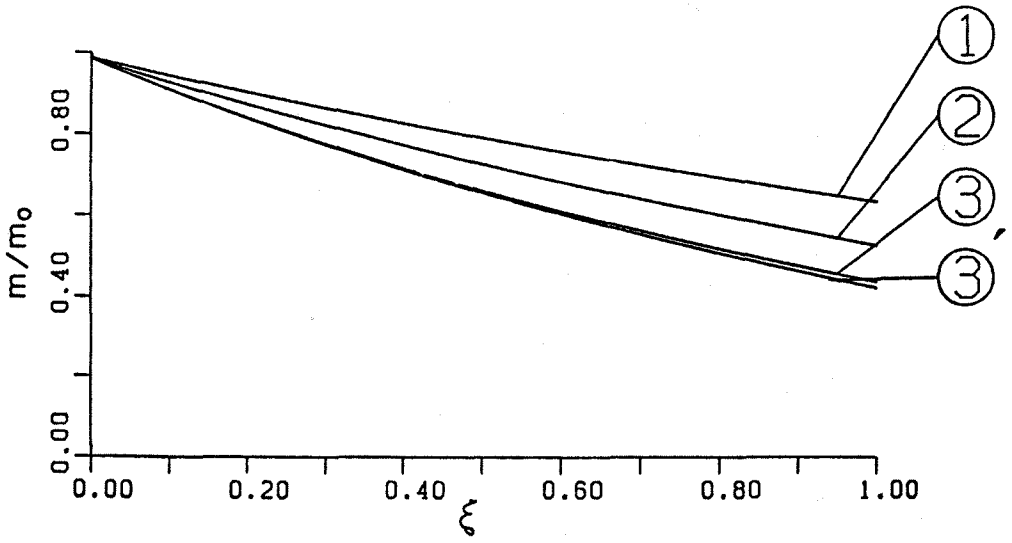

Fig. 5 Variations of weights vs. nondimensional distance.

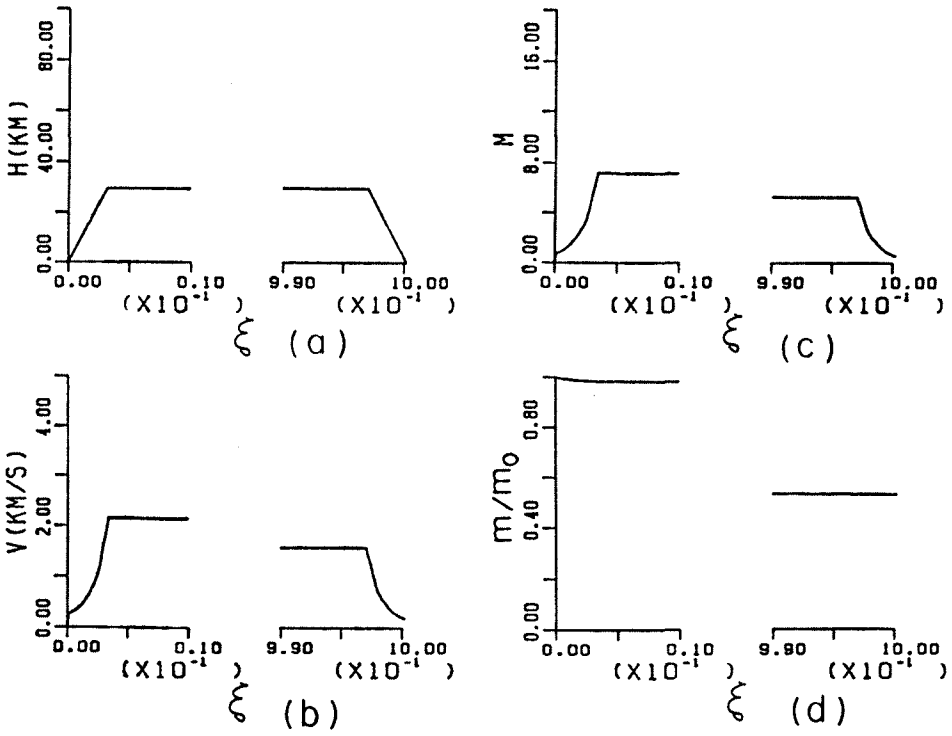

Fig. 6 Take-off and landing characteristics in case ②.
(a) Flight path. (b) Flight speed. (c) Mach number and (d) Weight.

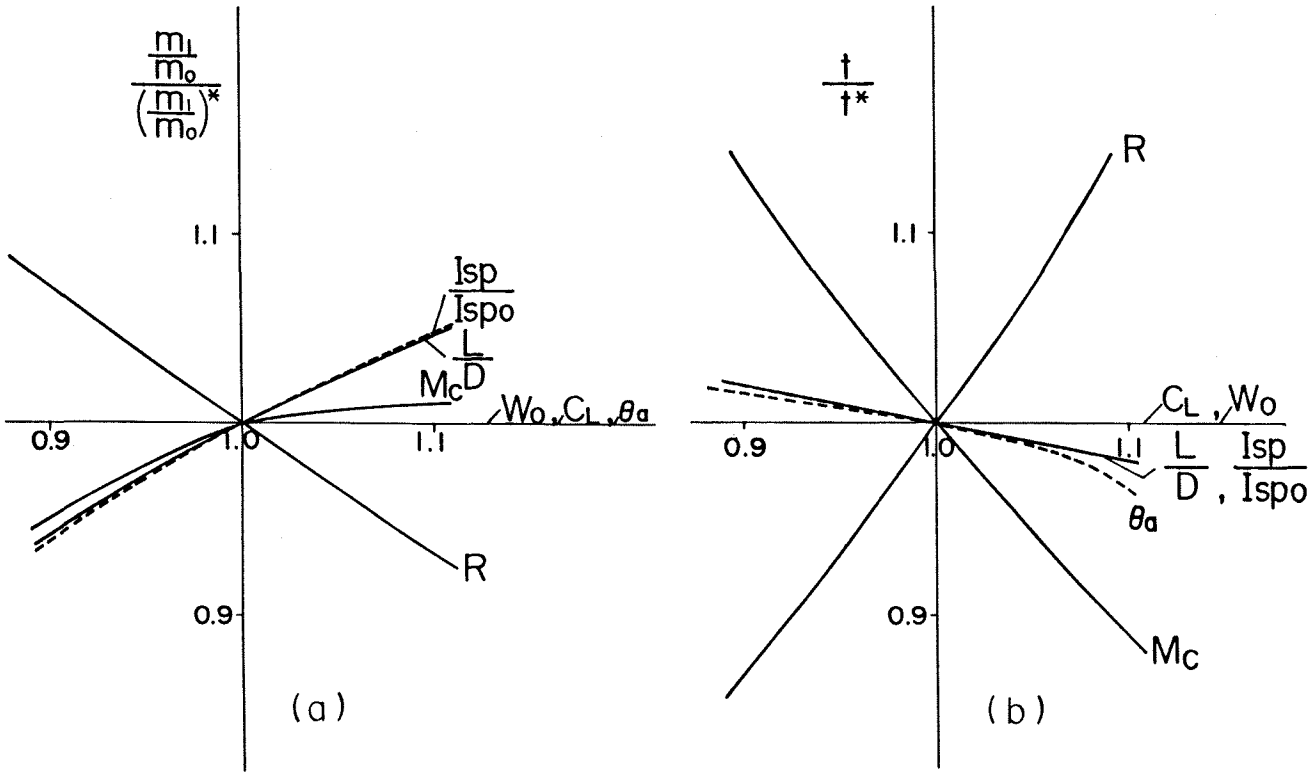

Fig. 7 Effect of design parameters in case ② (*).
(a) Weight change. (b) Flight time.

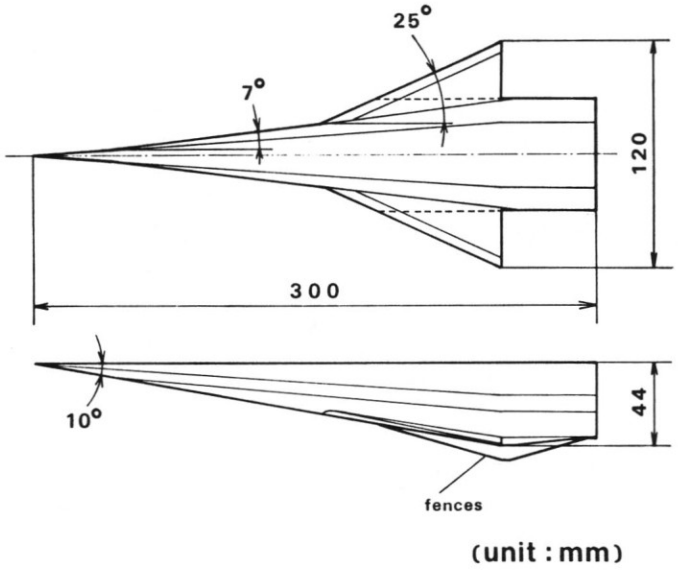

Fig. 8 Basic configuration of HST.

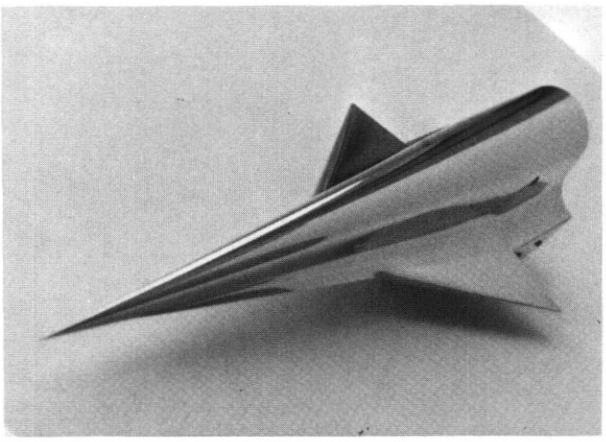

Fig. 9 Wind tunnel model of HST.

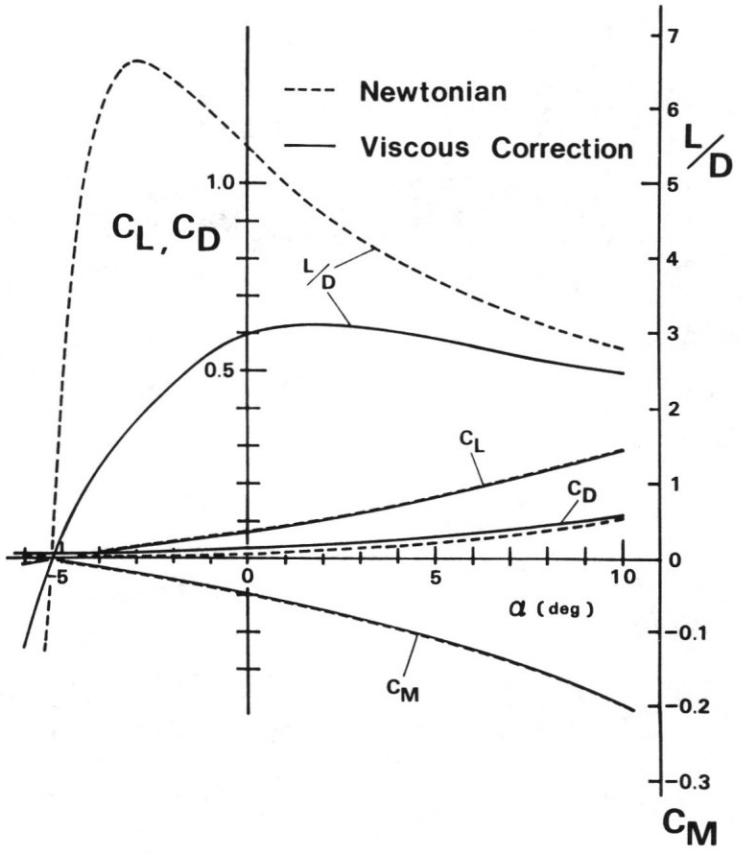

(a)

Fig. 10 Aerodynamic characteristics of the HST model at M = 7.10 and Re = 3.2×10^6. (a) Analysis. (b) Experiment.

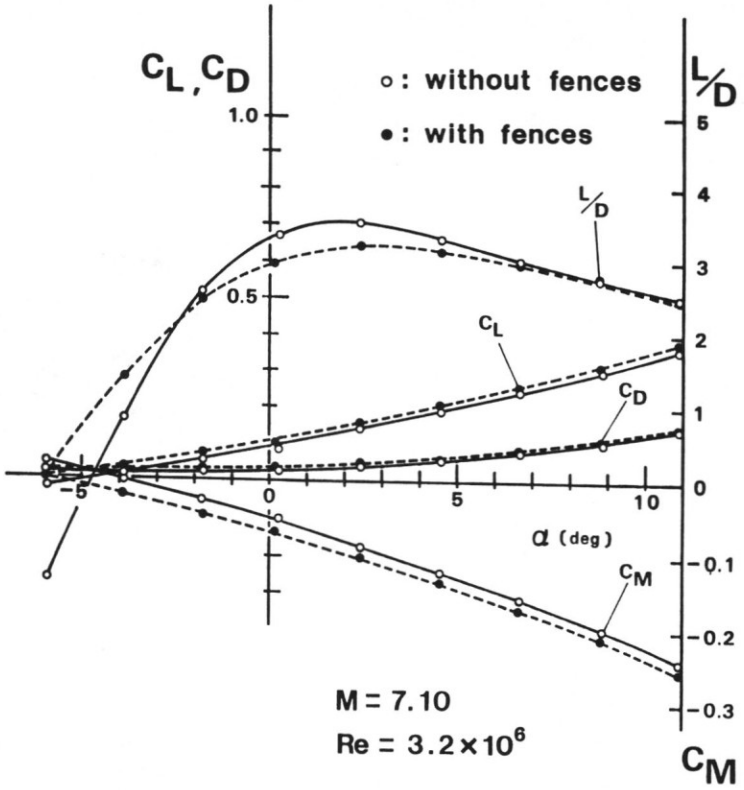

Fig. 10 (b)

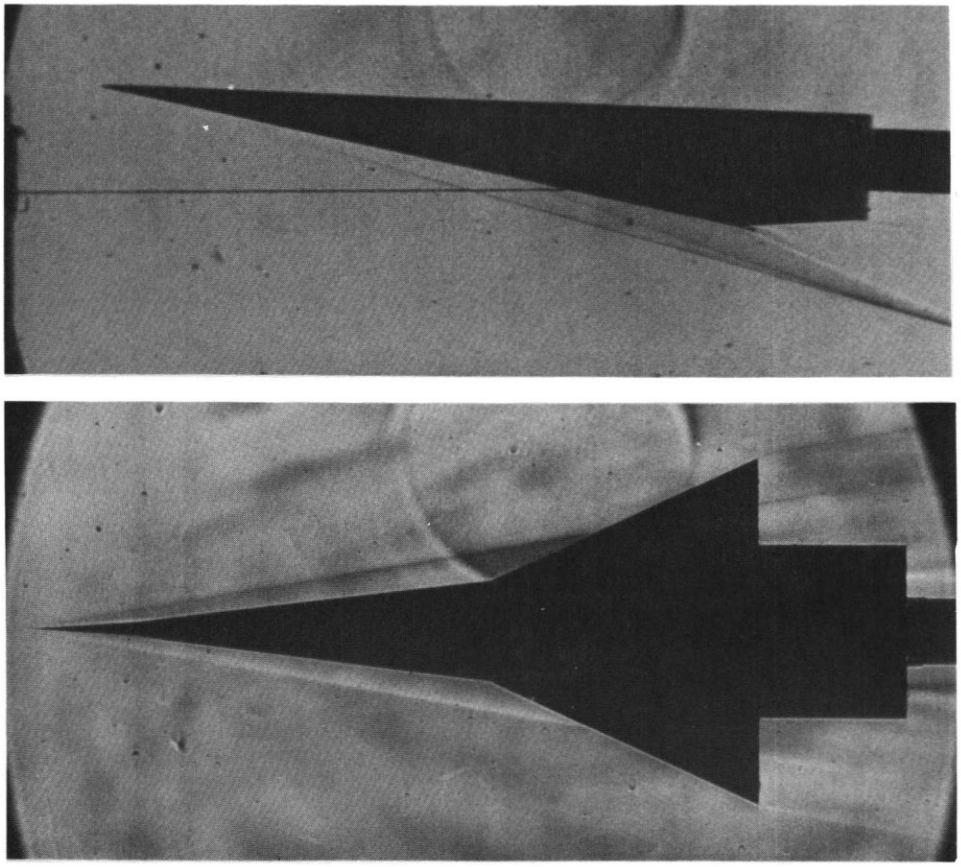

Fig. 11 Schlieren photograph of the flow around the HST model without fences (α = 2°).

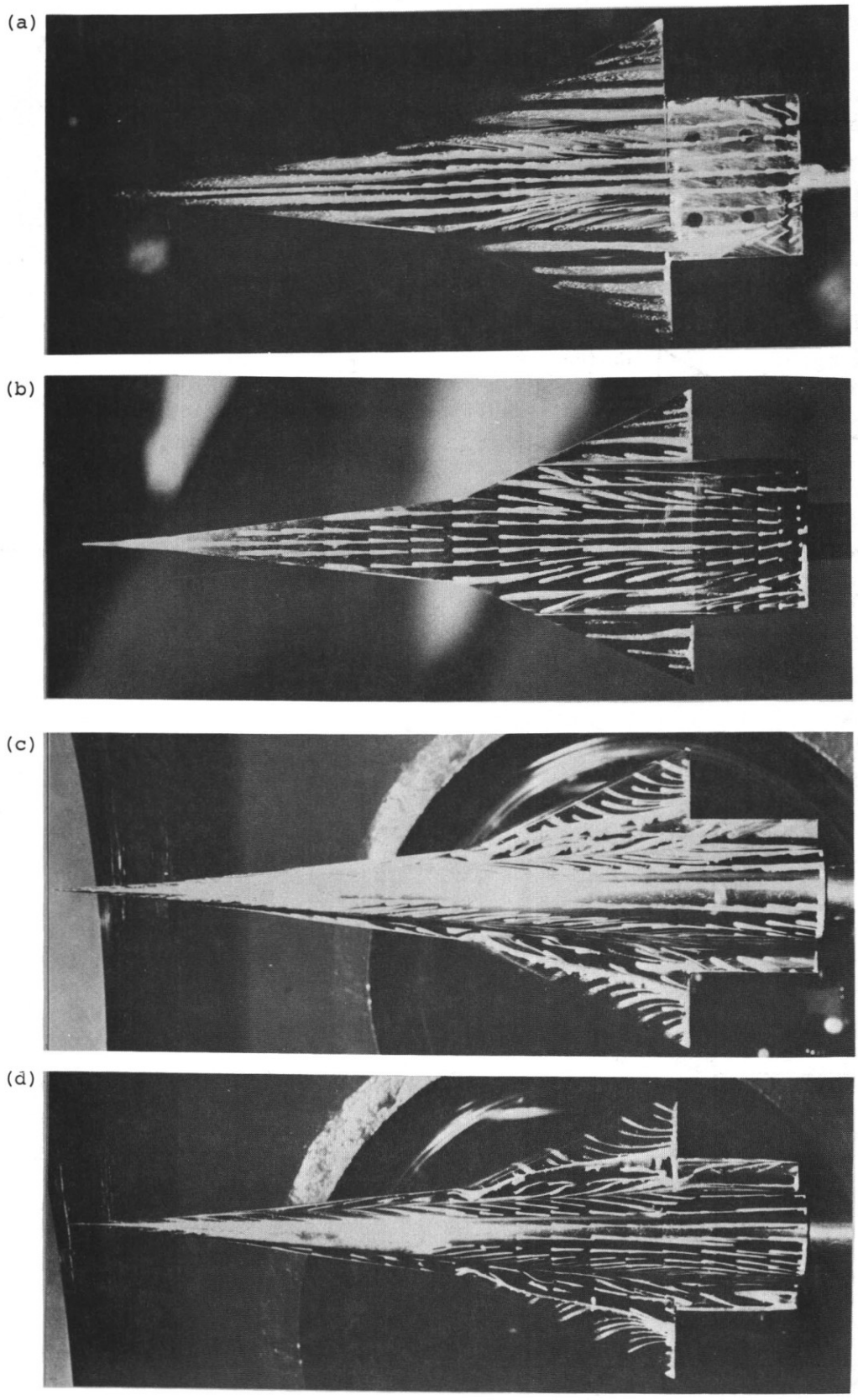

Fig. 12 Oil flow patterns.
(a) Lower surface, without fences.
(b) Lower surface, with fences.
(c) Upper surface, without fences.
(d) Upper surface, with fences.

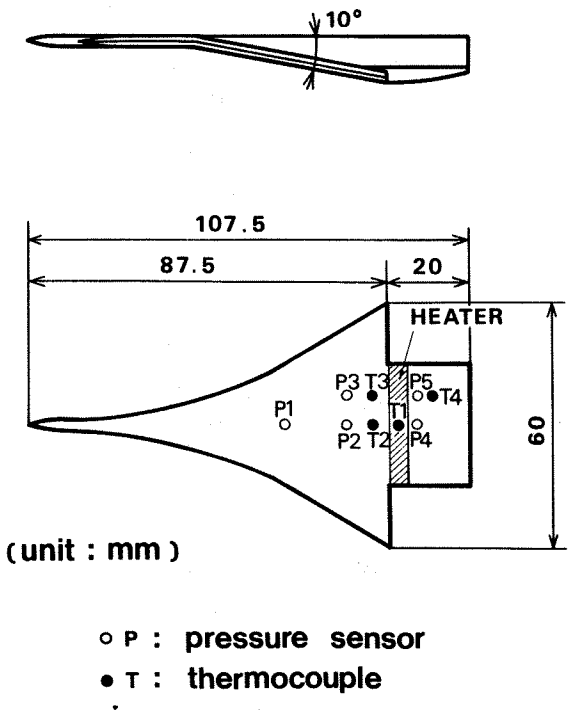

Fig. 13 Wind tunnel model of heat addition.

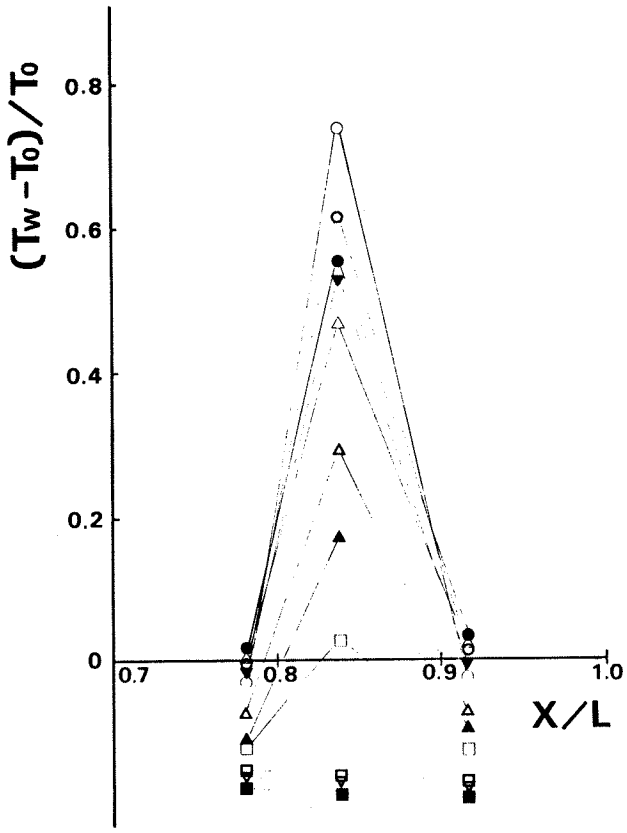

Fig. 14 Surface temperature distributions at several T_w.

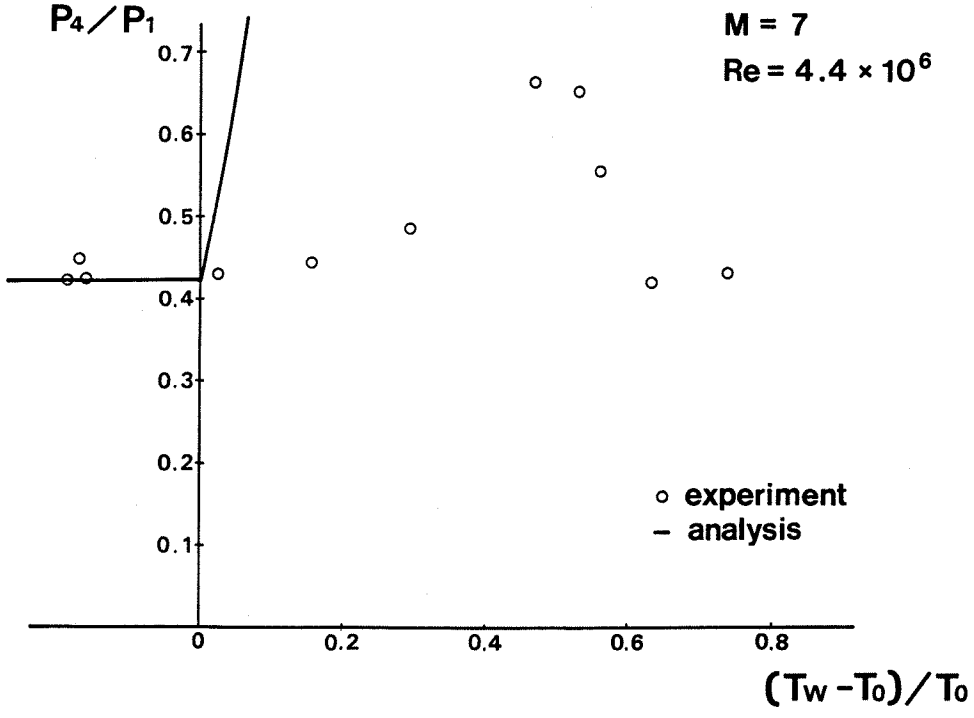

Fig. 15 Pressure change on the afterbody due to heat addition.